

Fermionic entanglement in altermagnets

M. Kulig,¹ T. Masłowski¹, K. A. Kouzakov², V. K. Dugaev¹, P. Kurashvili³, S. Wolski,¹
M. Inglot¹, C. Jasiukiewicz¹ and L. Chotorlishvili^{1,2}

¹*Department of Physics and Medical Engineering, Rzeszów University of Technology, 35-959 Rzeszów, Poland*

²*Faculty of Exact and Natural Sciences, Tbilisi State University, Chavchavadze av.3, 0128 Tbilisi, Georgia*

³*National Centre for Nuclear Research, Warsaw 00-681, Poland*



(Received 17 October 2024; revised 5 April 2025; accepted 8 May 2025; published 21 May 2025)

Altermagnetism became very popular because of unique features, namely coupling between magnetic properties and momentum of itinerant electrons. The particular model of the altermagnetic system of our interest has already been studied in recent publications in a different context: [Phys. Rev. B **108**, L140408 \(2023\)](#). Here, we study the scattering process of an itinerant electron from the altermagnetic material on the electron localized in a GaAs quantum dot doped on the altermagnetic material. We found a spatially inhomogeneous distribution of quantum entanglement in the postscattering state. An interesting observation is the spatially anisotropic distribution of concurrence which depends on the values of the altermagnetic spin-orbit interaction constant. We also studied Rényi entropy and the effect of disorder in the system leading to randomness in the spin-orbit constant. Our main finding is that, due to the unique properties of an altermagnetic system, tuning the applied external magnetic field allows tailoring of the desired entangled state. Thus the scattering process, in essence, mimics the Hadamard-CNOT gate transformation, converting the initial disentangled state into the entangled state of Bell's state. In particular, we achieved more than 70% fidelity between the postscattering and Bell's states.

DOI: [10.1103/PhysRevB.111.184427](https://doi.org/10.1103/PhysRevB.111.184427)

I. INTRODUCTION

The linearity of the Schrödinger equation leads to the superposition principle, a fundamental principle of quantum mechanics. Due to the superposition principle, the linear combinations of solutions also satisfy the Schrödinger equation. The superposition principle and quantumness of the system form the basis of the functionality of quantum computers and it has certain advantages. The list of proposed quantum registers for quantum computers is pretty long. It includes, e.g., superconducting quantum computing with Josephson junction qubits, trapped ions, and quantum dots [1–6]. The quantum register is a repository of qubits with quick access to them and the possibility of controlling their states through the quantum gates. In particular, semiconductor quantum dots attract the attention of the quantum information community [7–9]. Quantum dots (QD) in the materials with a strong spin-orbit (SO) interaction (graphene, carbon nanotubes, and topological insulators [10]) are in the scope of interest [11–15]. Spin-orbit interaction (SOI) can be exploited to increase the fidelity of quantum gates [16,17]. Recently, the study of altermagnetism became a hot topic [18–22]. Altermagnetic materials, such as insulators FeF₂ and MnF₂, semiconductors MnTe, and metals RuO₂, are characterized by magnetic properties strongly coupled with the momentum of the electrons. Coupling

between electronic and magnetic properties opens a new possibility for controlling qubits in QDs through the SOI and itinerant electron states. Altermagnets are viewed as a new type of magnetic material [18,19,23–26]. The main peculiarity of the altermagnetic state is the existence of spin splitting of electron energy bands, which is generated by the usual antiferromagnetic ordering in the magnetic sublattice (see, e.g., review articles [27,28]). The spin splitting is quite unusual for conventional antiferromagnets and is due to the specific orientational symmetry of electron orbitals, so that the band electrons moving in different directions experience the magnetization of different magnetic sublattices [18,28,29]. It was found that the symmetry of certain crystals like, e.g., RuO₂, MnTe, etc. allows such an altermagnetic state [20,29–33].

The spin splitting in altermagnets has some similarity to the spin splitting due to relativistic spin-orbit interaction and, correspondingly, makes it possible to use altermagnets in various spintronic applications. For instance, the existence of anomalous Hall effect, spin current generation, spin Seebeck and spin Nernst effects, *et al.* in the altermagnets was demonstrated [31–37]. In this work, we demonstrate that the nonrelativistic coupling of spin to the orbital motion in altermagnets can be also used for manipulating the quantum entanglement by using the scattering of electrons from the quantum dot. In particular, we consider altermagnetic material with doped GaAs quantum dot.

A disentangled bipartite system $|\psi\rangle_{AB} = |0\rangle_A \otimes |0\rangle_B$ can be entangled by performing a unitary quantum gate operation: $\text{CNOT}_{AB} \circ \text{Hadamard}_A |0\rangle_A |0\rangle_B = |\Phi\rangle_{AB}^+$, where $|\Phi\rangle_{AB}^+$ is the Bell's state. While the formal procedure is relatively straightforward, its implementation for the realistic physical system is

Published by the American Physical Society under the terms of the [Creative Commons Attribution 4.0 International](#) license. Further distribution of this work must maintain attribution to the author(s) and the published article's title, journal citation, and DOI.

a demanding problem. One practical realization of the entangling gate procedure is the elastic spin-dependent scattering protocol [38–41]. A unitary scattering \hat{S} matrix converting a disentangled state into an entangled postscattering state can be viewed as the equivalent of the Hadamard and CNOT gates $\hat{S} \equiv \{\text{CNOT}_{AB} \circ \text{Hadamard}_A\}$.

It connects the initial disentangled bipartite state with a final entangled state $|\Psi_{AB}^f(\infty)\rangle = \hat{S}|\Psi_{AB}^i(-\infty)\rangle$. One of the methods for the generation of entangled pairs of electrons is a scattering process [41–50]. In the present work, we study the scattering process of the itinerant electron of the altermagnetic system on the electron localized in the quantum dot, which is deposited on the surface of an altermagnet. We prove that the scattering of two electrons leads to the formation of the entangled state due to the features of the altermagnetic system. The key role belongs to the coupling between electronic and magnetic properties and the presence of a SOI effect in the altermagnetic system.

Measuring the entanglement in the experiments is related to specific dilemmas. Let \hat{O} be an arbitrary Hermitian quantum operator and $\text{Tr}(\hat{\rho}\hat{O})$ the expectation value of it averaged through the density matrix of the system $\hat{\rho}$. Then nonlinear functions of the density matrix, i.e., purity $\text{Tr}(\hat{\rho}^2)$, can be measured directly without reconstruction of the whole density matrix $\hat{\rho}$ [51–54]. There are two different direct and indirect measurement schemes. The direct measurement scheme implies n identical copies of the quantum systems prepared in the same state $\hat{\rho}$. Measurements are performed on those multiple copies. In many cases, it is a “thought experiment,” since the noncloning theorem does not permit copying and preparing a desired number of the identical quantum states. The elegant solution is a random measurement that only implies a single copy of $\hat{\rho}$ [55,56]. One applies the random unitary rotation operator \hat{U} to a single copy of the state $\hat{U}\hat{\rho}_{AB}\hat{U}^{-1}$, where $\hat{\rho}_{AB} = |\Psi\rangle\langle\Psi|_{AB}$ is the density matrix of the bipartite system. Then, the result is averaged over random unitaries. In essence, the ensemble average of a single random measurement is equivalent to the set of deterministic measurements [55,56]. In our case, the practical implementation of the random unitary rotation operator is equivalent to the random SOI in the scattering problem. Randomness in the SOI is related to the disorder and impurities and is a realistic assumption for two-dimensional solid-state materials [13,57]. In what follows, we will be focused on Renyi entropies, which can be determined from a tomographic reconstruction of the quantum state [58–61] and measured experimentally [62,63]: $S^{(n)}(\hat{\rho}_A) = [1/(n-1)] \log \text{Tr}(\hat{\rho}_A^n)$, where $\hat{\rho}_A$ is the reduced matrix $\hat{\rho}_A = \text{Tr}_B(\hat{\rho}_{AB})$ of the part A . We are interested in outcome probabilities $P(s) = \text{Tr}[\hat{U}\hat{\rho}_A\hat{U}^\dagger\mathcal{P}_s]$, where $\mathcal{P}_s = |s\rangle\langle s|$ are projectors and \hat{U} is the random unitary matrix. Then Renyi entropy is extracted through the statistical moments

$$\langle P(s)^n \rangle = \langle \text{Tr}[(\hat{U}\hat{\rho}_A\hat{U}^\dagger)^{\otimes n}\mathcal{P}_s^{\otimes n}] \rangle, \quad (1)$$

where $\langle \dots \rangle$ means averaging over disorder. We consider a bipartite system consisting of an altermagnet (itinerant electron \mathbf{A}) and quantum dot (localized electron \mathbf{B}) prepared initially in a product state. We assume the randomness of the SO coupling constant (due to the disorder and impurities that may exist in the realistic material). We tackle the elastic

scattering process as a random unitary operation and explore the entanglement of the scattered state. Thus random unitaries in our proposal are replaced by a random SOI elastic scattering process $\hat{U} = \hat{S}$. We calculate fidelity $\mathcal{F}(|\Psi_{AB}^f(\infty)\rangle, |\Psi_{AB}^i(-\infty)\rangle)$ between scattered state $|\Psi_{AB}^f(\infty)\rangle = \hat{S}|\Psi_{AB}^i(-\infty)\rangle$ and the state obtained through the applied gate $|\Psi_{AB}^i(-\infty)\rangle = \{\text{CNOT}_{AB} \circ \text{Hadamard}_A\}|\Psi_{AB}^i(-\infty)\rangle$.

We present results for fermionic entanglement as a function of momentum of itinerant electron \mathbf{k} . The scattered electron with particular \mathbf{k} is singled out of all the other electrons forming the altermagnet due to the Pauli principle. Other itinerant electrons in altermagnet are not allowed to have the same momentum \mathbf{k} . However, this does not mean that our result applies only to a single particular electron case. We present results for different \mathbf{k} corresponding to the ensemble of itinerant electrons in an altermagnet. We follow the Lippmann-Schwinger formalism of the scattering problem. Formulated for a single electron, this formalism describes the scattering problem of the ensemble of electrons with different \mathbf{k} . Our aim is to find particular electrons forming entangled pairs with the electron from the quantum dot. A quantum dot is deposited on the altermagnet. The electron from the altermagnet is not far away from the electron in the quantum dot. The distance between electrons is about magnetic localization length, in the range of the radius of the quantum dot. Therefore, entangled pairs of electrons in the system altermagnet-quantum dot form a prototype repository for storing quantum information. The paper is organized as follows. In Sec. II, we solve the scattering problem; in Sec. III, we present results for concurrence obtained for the deterministic SO coupling constant. The Rényi entropy is discussed in Sec. IV. Section V concludes the work.

II. SCATTERING PROBLEM

Recently, there has been a growing interest in the problem of magnetic impurities in altermagnets [64–70]. In essence, in the following discussion we formulate the problem theoretically and develop a mathematical description of the scattering problem relevant to quantum dots characterized by the SO coupling. The total Hamiltonian of the system comprises the three terms

$$\hat{H}_{\text{tot}} = \hat{H}_{AM} + \hat{H}_D + \hat{V}. \quad (2)$$

Here $\hat{H}_{AM} = \varepsilon_k + \alpha_e \hat{\sigma}_A^z k_x k_y$, $k_x = k \cos \theta$, $k_y = k \sin \theta$ is the low-energy Hamiltonian for the altermagnet, $\varepsilon_k = \hbar^2 k^2 / 2m$, $\hat{\sigma}_A^z$ is the Pauli operator for the spin of itinerant electron, k is the momentum of itinerant electron, and α_e is the SOI constant [71]. The Hamiltonian of the electron localized in the doped GaAs quantum dot (QD) has the form

$$\hat{H}_D = -B\hat{\sigma}_B^z + \frac{\hbar^2}{2m_e} \left(-i\nabla + \frac{e}{\hbar}\mathbf{A} \right)^2 + \frac{1}{2}m\omega_0^2 r^2, \quad (3)$$

where ω_0 is the frequency of electron oscillation in QD, m_e is the effective mass, and \mathbf{A} is the vector potential. In particular, for GaAs QD we consider the following parameters: the effective mass $m_e = 0.067m$ (m is the electron mass), g factor $g = -0.44$, and the confinement energy $\hbar\omega_0 = 4.4$ meV. The external magnetic field applied locally to the quantum dot allows it to freeze (strong field) or relax (weak field) the spin

of the localized electron $\hat{\sigma}_B^z$ depending on the value of Zeeman energy $B \equiv \hbar\gamma_e B$. The lowest Fock-Darwin eigenstate of the localized electron in the symmetric gauge $\mathbf{A} = B(-y, x, 0)/2$ has the form [72]

$$\psi_D(\mathbf{r}) = \frac{1}{l_B\sqrt{\pi}} \exp\left(-\frac{x^2 + y^2}{2l_B^2}\right),$$

$$l_B^2 = l_0^2/\sqrt{1 + B^2 e^2 l_0^4/4\hbar^2}. \quad (4)$$

Here $l_0 = (\hbar/m_e\omega_0)^{1/2}$ is the confinement length [73]. Hereafter we set dimensionless $\mathbf{r} \equiv \mathbf{r}/l_0$ and measure the distance in terms of the confinement length. The last term in Eq. (2) describes the interaction between localized and itinerant electrons. We consider the short range interaction case [74]:

$$\hat{V} = J \hat{\sigma}_A \cdot \hat{\sigma}_B \delta(\mathbf{r}_1 - \mathbf{r}_2). \quad (5)$$

The coupling constant J is determined by the ratio [75] $J \approx T^2/U$, where U and T are the Coulomb interaction and electron hopping terms:

$$U = \frac{e^2}{4\pi\epsilon_0 l_0} \int \frac{|\psi_{n,\sigma}(\mathbf{r}_1)|^2 |\psi_{D,\sigma}(\mathbf{r}_2)|^2}{|\mathbf{r}_1 - \mathbf{r}_2| + \delta} d\mathbf{r}_1 d\mathbf{r}_2,$$

$$T = E \int \psi_{n,\sigma}^\dagger(\mathbf{r}) \psi_{D,\sigma}(\mathbf{r}) d\mathbf{r}. \quad (6)$$

Here $\hat{\sigma}_B$ refers to the Pauli vector of the spin of quantum dot and δ is the cutoff of electron-electron interaction, $\hat{\sigma}_A$ is the Pauli vector of the spin of itinerant electron in altermagnet, and R is the radius of the quantum dot.

The initial wave function of the bipartite system is a product of two wave functions $\psi_{n,\sigma}(\mathbf{r}_A)$ and $\psi_{D,\sigma}(\mathbf{r}_B) = \psi(\mathbf{r}_B)|0\rangle_B$. In what follows, for brevity, we use the notations $\mathbf{r}_A \equiv \mathbf{r}$ and $\mathbf{r}_B \equiv \mathbf{r}'$. The scattering process involves two states of localized electron $\psi_{D,0}(\mathbf{r}) = \psi_D(\mathbf{r})|0\rangle$ (spin-up, $|0\rangle \equiv |\uparrow\rangle$) and $\psi_{D,1}(\mathbf{r}) = \psi_D(\mathbf{r})|1\rangle$; spin-down, $|1\rangle \equiv |\downarrow\rangle$). The wave function of the two-electron system after scattering can be presented in the following general form:

$$\Psi_{\sigma_1\sigma_2}(\mathbf{r}_1, \mathbf{r}_2) = \psi_0^{(+)}(\mathbf{r}_1)\psi_{D,0}(\mathbf{r}_2) + \psi_1^{(+)}(\mathbf{r}_1)\psi_{D,1}(\mathbf{r}_2). \quad (7)$$

Here $\psi_{n,0}^{(+)}$ and $\psi_{n,1}^{(+)}$ are the two-component spinors

$$\psi_0^{(+)}(\mathbf{r}) = \begin{pmatrix} \phi_0(\mathbf{r}) \\ \chi_0(\mathbf{r}) \end{pmatrix}, \quad \psi_1^{(+)}(\mathbf{r}) = \begin{pmatrix} \phi_1(\mathbf{r}) \\ \chi_1(\mathbf{r}) \end{pmatrix}. \quad (8)$$

In the momentum-space representation,

$$\psi_{0(1)}^{(+)}(\mathbf{p}) = \int d^2r e^{-i\mathbf{p}\mathbf{r}} \psi_{0(1)}^{(+)}(\mathbf{r}),$$

spinors in the above equation are the solution of the following system of coupled Lippmann-Schwinger integral equations ($n = \mathbf{k}, \sigma = \uparrow$):

$$\begin{pmatrix} \phi_0(\mathbf{p}) \\ \chi_0(\mathbf{p}) \end{pmatrix} = (2\pi)^2 \delta(\mathbf{p} - \mathbf{k}) \left[\alpha \begin{pmatrix} 1 \\ 0 \end{pmatrix} + \beta \begin{pmatrix} 0 \\ 1 \end{pmatrix} \right]$$

$$+ \alpha \int \frac{d^2q}{(2\pi)^2} \hat{G}^{(+)}(\mathbf{p}; E) \hat{V}_{00}(q) \begin{pmatrix} \phi_0(\mathbf{p} - \mathbf{q}) \\ \chi_0(\mathbf{p} - \mathbf{q}) \end{pmatrix}$$

$$+ \beta \int \frac{d^2q}{(2\pi)^2} \hat{G}^{(+)}(\mathbf{p}; E) \hat{V}_{01}(q) \begin{pmatrix} \phi_1(\mathbf{p} - \mathbf{q}) \\ \chi_1(\mathbf{p} - \mathbf{q}) \end{pmatrix} \quad (9)$$

and

$$\begin{pmatrix} \phi_1(\mathbf{p}) \\ \chi_1(\mathbf{p}) \end{pmatrix} = \alpha \int \frac{d^2q}{(2\pi)^2} \hat{G}^{(+)}(\mathbf{p}; E - 2B) \hat{V}_{10}(q) \begin{pmatrix} \phi_0(\mathbf{p} - \mathbf{q}) \\ \chi_0(\mathbf{p} - \mathbf{q}) \end{pmatrix}$$

$$+ \beta \int \frac{d^2q}{(2\pi)^2} \hat{G}^{(+)}(\mathbf{p}; E - 2B) \hat{V}_{11}(q) \begin{pmatrix} \phi_1(\mathbf{p} - \mathbf{q}) \\ \chi_1(\mathbf{p} - \mathbf{q}) \end{pmatrix}. \quad (10)$$

The Green's function has the form

$$\hat{G}^{(+)}(\mathbf{p}; E) = \frac{1}{2} \frac{\hat{I} + \hat{\sigma}_z}{E - E_{\mathbf{k},\uparrow} + i0} + \frac{1}{2} \frac{\hat{I} - \hat{\sigma}_z}{E - E_{\mathbf{k},\downarrow} + i0}, \quad (11)$$

where $E_{\mathbf{k},\uparrow,\downarrow} = \varepsilon_{\mathbf{k}} \pm \alpha_e k_x k_y$ and matrix elements read $\hat{V}_{00}(\mathbf{q}) = J e^{-q^2 l_B^2/2} \hat{\sigma}_z$, $\hat{V}_{01}(\mathbf{q}) = J e^{-q^2 l_B^2/2} (\hat{\sigma}_x - i\hat{\sigma}_y)$, $\hat{V}_{10}(\mathbf{q}) = J e^{-q^2 l_B^2/2} (\hat{\sigma}_x + i\hat{\sigma}_y)$, and $\hat{V}_{11}(\mathbf{r}_A) = -J e^{-q^2 l_B^2/2} \hat{\sigma}_z$. Details of the calculation of integrals are presented in the Appendix Eqs. (A1)–(A15).

III. POSTSCATTERING DENSITY MATRIX

In the spirit of the scattering theory, we present the postscattering density matrix in terms of the spatial coordinates, energy, and spin of the itinerant electron. Consequently, the entanglement between the electrons depends on the same parameters. Thus we can preselect and propose particular initial itinerant electrons that, after scattering, are entangled stronger with localized electrons rather than other electrons. Taking into account the initial density matrix

$$\hat{\rho}_0 = |\psi_{T,\sigma}(\mathbf{r})\psi_D\rangle \langle \psi_{T,\sigma}(\mathbf{r})\psi_D| \otimes |0\rangle \langle 0|_B \quad (12)$$

and the wave function of the system after scattering Eq. (7), we define two random unitary matrices through the following formulas:

$$\hat{\rho} = |\Psi_{\sigma_1\sigma_2}(\mathbf{r}, \mathbf{r}')\rangle \langle \Psi_{\sigma_1\sigma_2}(\mathbf{r}, \mathbf{r}')| = \hat{U} \hat{\rho}_0 \hat{U}^\dagger, \quad (13)$$

$$\hat{\rho}_A = \hat{U}_A \hat{\rho}_0 \hat{U}_A^\dagger. \quad (14)$$

Here index \mathbf{A} means that gate transformation \hat{U}_A acts only on the qubit \mathbf{A} , while the qubit of the localized electron \mathbf{B} is frozen by applied strong magnetic field. The explicit form of the density matrices read

$$\hat{\rho} = \rho_{11} |0\rangle \langle 0|_A \otimes |0\rangle \langle 0|_B + \rho_{22} |1\rangle \langle 1|_A \otimes |0\rangle \langle 0|_B$$

$$+ \rho_{44} |1\rangle \langle 1|_A \otimes |1\rangle \langle 1|_B + \rho_{12} |0\rangle \langle 1|_A \otimes |0\rangle \langle 0|_B$$

$$+ \rho_{14} |0\rangle \langle 1|_A \otimes |0\rangle \langle 1|_B + \rho_{21} |1\rangle \langle 0|_A \otimes |0\rangle \langle 0|_B$$

$$+ \rho_{41} |1\rangle \langle 0|_A \otimes |1\rangle \langle 0|_B + \rho_{24} |1\rangle \langle 1|_A \otimes |0\rangle \langle 1|_B$$

$$+ \rho_{42} |1\rangle \langle 1|_A \otimes |1\rangle \langle 0|_B, \quad (15)$$

where

$$\begin{aligned}\rho_{11} &= \frac{\alpha^2 |e^{i\mathbf{k}\mathbf{r}} + JI_1(\mathbf{r})|^2}{\alpha^2 |e^{i\mathbf{k}\mathbf{r}} + JI_1(\mathbf{r})|^2 + \beta^2 + \beta^2 J^2 |I_2(\mathbf{r})|^2}, \\ \rho_{22} &= \frac{\beta^2}{\alpha^2 |e^{i\mathbf{k}\mathbf{r}} + JI_1(\mathbf{r})|^2 + \beta^2 + \beta^2 J^2 |I_2(\mathbf{r})|^2}, \\ \rho_{44} &= \frac{\beta^2 J^2 |I_2(\mathbf{r})|^2}{\alpha^2 |e^{i\mathbf{k}\mathbf{r}} + JI_1(\mathbf{r})|^2 + \beta^2 + \beta^2 J^2 |I_2(\mathbf{r})|^2},\end{aligned}\quad (16)$$

and

$$\begin{aligned}\rho_{12} &= \frac{\alpha\beta[1 + J e^{-i\mathbf{k}\mathbf{r}} I_1(\mathbf{r})]}{\alpha^2 |e^{i\mathbf{k}\mathbf{r}} + JI_1(\mathbf{r})|^2 + \beta^2 + \beta^2 J^2 |I_2(\mathbf{r})|^2}, \\ \rho_{14} &= \frac{\alpha\beta J I_2^*(\mathbf{r}) [e^{i\mathbf{k}\mathbf{r}} + JI_1(\mathbf{r})]}{\alpha^2 |e^{i\mathbf{k}\mathbf{r}} + JI_1(\mathbf{r})|^2 + \beta^2 + \beta^2 J^2 |I_2(\mathbf{r})|^2}, \\ \rho_{24} &= \frac{\beta^2 J e^{i\mathbf{k}\mathbf{r}} I_2^*(\mathbf{r})}{\alpha^2 |e^{i\mathbf{k}\mathbf{r}} + JI_1(\mathbf{r})|^2 + \beta^2 + \beta^2 J^2 |I_2(\mathbf{r})|^2},\end{aligned}\quad (17)$$

$\rho_{12} = \rho_{21}^*$, $\rho_{14} = \rho_{41}^*$, and $\rho_{24} = \rho_{42}^*$. For the second matrix we deduce

$$\begin{aligned}\hat{\rho}_A &= \rho_{A11} |0\rangle \langle 0|_A \otimes |0\rangle \langle 0|_B + \rho_{A22} |1\rangle \langle 1|_A \otimes |0\rangle \langle 0|_B \\ &\quad + \rho_{A12} |0\rangle \langle 1|_A \otimes |0\rangle \langle 0|_B + \rho_{A21} |1\rangle \langle 0|_A \otimes |0\rangle \langle 0|_B,\end{aligned}\quad (18)$$

and

$$\begin{aligned}\rho_{A11} &= \frac{\alpha^2 |e^{i\mathbf{k}\mathbf{r}} + JI_1(\mathbf{r})|^2}{\alpha^2 |e^{i\mathbf{k}\mathbf{r}} + JI_1(\mathbf{r})|^2 + \beta^2}, \\ \rho_{A22} &= \frac{\beta^2}{\alpha^2 |e^{i\mathbf{k}\mathbf{r}} + JI_1(\mathbf{r})|^2 + \beta^2}, \\ \rho_{A12} &= \frac{\alpha\beta[1 + J e^{-i\mathbf{k}\mathbf{r}} I_1(\mathbf{r})]}{\alpha^2 |e^{i\mathbf{k}\mathbf{r}} + JI_1(\mathbf{r})|^2 + \beta^2},\end{aligned}\quad (19)$$

and $\rho_{A12} = \rho_{A21}^*$.

IV. CONCURRENCE AND FIDELITY

We exploit the definition of concurrence [76] $\mathcal{C} = |\langle \psi | \hat{\sigma}_y \otimes \hat{\sigma}_y | \psi^* \rangle|$, where $\hat{\sigma}_y \otimes \hat{\sigma}_y$ is the direct product of Pauli matrices, and calculate entanglement between two electrons after scattering:

$$\mathcal{C} = \frac{2\alpha\beta J |e^{-i\mathbf{k}\mathbf{r}} + JI_1^*(\mathbf{r}) I_2^*(\mathbf{r})|}{\alpha^2 |e^{i\mathbf{k}\mathbf{r}} + JI_1(\mathbf{r})|^2 + \beta^2 + \beta^2 J^2 |I_2(\mathbf{r})|^2}.\quad (20)$$

In what follows we explore concurrence in the absence of disorder. For the fidelity between Bell's state $|\Phi\rangle_{AB}^+$ and scattered

state $\hat{\rho}$ we deduce

$$\mathcal{F}(\hat{\rho}, |\Phi\rangle_{AB}^+) = \frac{1}{2}(\rho_{11} + \rho_{44} + \rho_{14} + \rho_{41}).\quad (21)$$

When $\alpha = \beta$, $J = 1$, Eq. (21) takes the form

$$\begin{aligned}\mathcal{F}_{\alpha=\beta}(\hat{\rho}, |\Phi\rangle_{AB}^+) &= \frac{|I_4(\mathbf{r})|^2 + |I_2(\mathbf{r})|^2}{2[|I_4(\mathbf{r})|^2 + |I_2(\mathbf{r})|^2 + 1]} \\ &\quad + \frac{\text{Re}[I_2^*(\mathbf{r}) I_4(\mathbf{r})]}{|I_4(\mathbf{r})|^2 + |I_2(\mathbf{r})|^2 + 1},\end{aligned}\quad (22)$$

where we introduced the notation $I_4(\mathbf{r}) = e^{i\mathbf{k}\mathbf{r}} + I_1(\mathbf{r})$. When $\alpha = 1$, $\beta = 0$ fidelity takes the value $\mathcal{F}(\hat{\rho}, |\Phi\rangle_{AB}^+) = 1/2$. In Fig. 1, we plot the spatially anisotropic distribution of entanglement $r_x = r \cos \varphi$, $r_y = r \sin \varphi$, for equally distributed spin up/down incident states $\alpha^2 = \beta^2 = 1/2$ of the itinerant electron beam. We present results for different θ : $k_x = k \cos \theta$, $k_y = k \sin \theta$, for zero and nonzero magnetic fields and other parameters as they are shown in the figure caption. As we see from Fig. 1 magnetic field B substantially enhances the value of concurrence, from $\mathcal{C}(\varphi) = 0.35$ up to the $\mathcal{C}(\varphi) = 0.9$. Besides, due to the strong SOI in the system, concurrence strongly depends on the momentum \mathbf{k} of the itinerant electron. We see an interesting physical effect in Fig. 2. Spatially anisotropic distribution of concurrence depends on the values of alternating SOI constant α_e . In the case of the weak SOI constant, the maximal value of concurrence is shifted towards small scattering angles, meaning $\varphi = 0, \pi$, $r_x \approx \pm r$, and $r_y \approx \pm 0$. In Fig. 3, we plot the spatially resolved anisotropic distribution of fidelity between the postscattering state and Bell's state $|\Phi\rangle_{AB}^+$, which is our desired target state. As we can see, akin to the concurrence, fidelity's maximal value rotates upon the change in the spin-orbit constant. Besides, the value of fidelity reaches 70%, which is a quite reasonable value for the gate $\{\text{Hadamard}_A \circ \text{CNOT}_B\}$.

V. RÉNYI ENTROPY

We proceed and calculate Rényi entropy of the bipartite system after scattering taking into account disorder in the system and randomness of the spin-orbit interaction constant. Following [77], we present the bipartite density matrix through the Pauli strings:

$$\begin{aligned}\hat{\rho} &= \frac{1}{4} \sum_{\mu, \nu=0}^3 \mathcal{R}_{\mu\nu} D_{\mu\nu}, \\ \mathcal{R}_{\mu\nu} &= \text{Tr}[\hat{\rho} D_{\mu\nu}], \quad \hat{\sigma}_0 = \mathcal{I}_{A,B}, \\ D_{\mu\nu} &= \hat{\sigma}_A^\mu \otimes \hat{\sigma}_B^\nu,\end{aligned}\quad (23)$$

where $D_{\mu\nu}$ is the Dirac matrix [78]. After laborious calculations we deduce

$$\mathcal{R} = \begin{bmatrix} 1 & 2 \text{Re}(\rho_{12}) & -2 \text{Im}(\rho_{12}) & \rho_{11}^2 - \rho_{22}^2 - \rho_{44}^2 \\ 2 \text{Re}(\rho_{24}) & 2 \text{Re}(\rho_{14}) & -2 \text{Im}(\rho_{14}) & -2 \text{Re}(\rho_{24}) \\ -2 \text{Im}(\rho_{24}) & -2 \text{Im}(\rho_{14}) & -2 \text{Re}(\rho_{14}) & 2 \text{Im}(\rho_{24}) \\ \rho_{11}^2 + \rho_{22} - \rho_{44} & 2 \text{Re}(\rho_{12}) & -2 \text{Im}(\rho_{12}) & \rho_{11}^2 + \rho_{22} + \rho_{44} \end{bmatrix}.\quad (24)$$

The quantity of interest, the second Rényi entropy, is given as

$$S_2(\hat{\rho}) = -\log_2 \text{Tr}[\hat{\rho}^2].\quad (25)$$

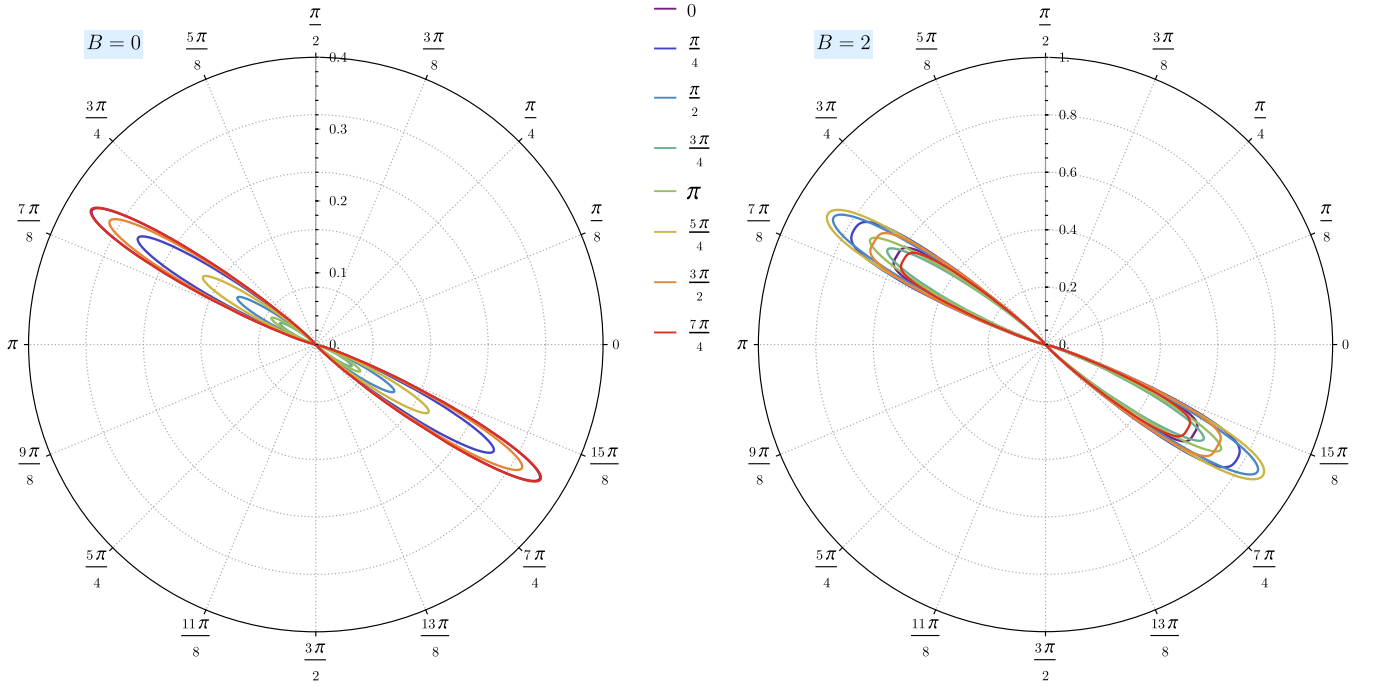


FIG. 1. Spatially anisotropic distribution of concurrence $\mathcal{C}(\varphi)$, in the polar coordinate system $r_x = r \cos \varphi$, $r_y = r \sin \varphi$, for equally distributed spin up/down incident states $\alpha^2 = \beta^2 = 1/2$ of the itinerant electron. We present results for different θ : $k_x = k \cos \theta$, $k_y = k \sin \theta$, for zero $B = 0$ (the left plot) and nonzero $B = 2$ T magnetic fields (the right plot). The values of parameters read $\hbar\omega_0 = 4.4$ meV, $U = 1$ meV, $J = 0.25$ meV, $\alpha_e/\alpha_c = 0.6$, $k \equiv l_0 k = 1$, $E = 15$ meV, $r \equiv r/l_0 = 10$, and $l_0 = (\hbar/m_e\omega_0)^{1/2}$ is the confinement length, $\alpha_c = \hbar^2/m_e$. The effective mass $m_e = 0.067m$ (m is the electron mass) and g factor $g = -0.44$, which leads to the $l_0 \approx 15$ nm. Different colors annotate values of θ .

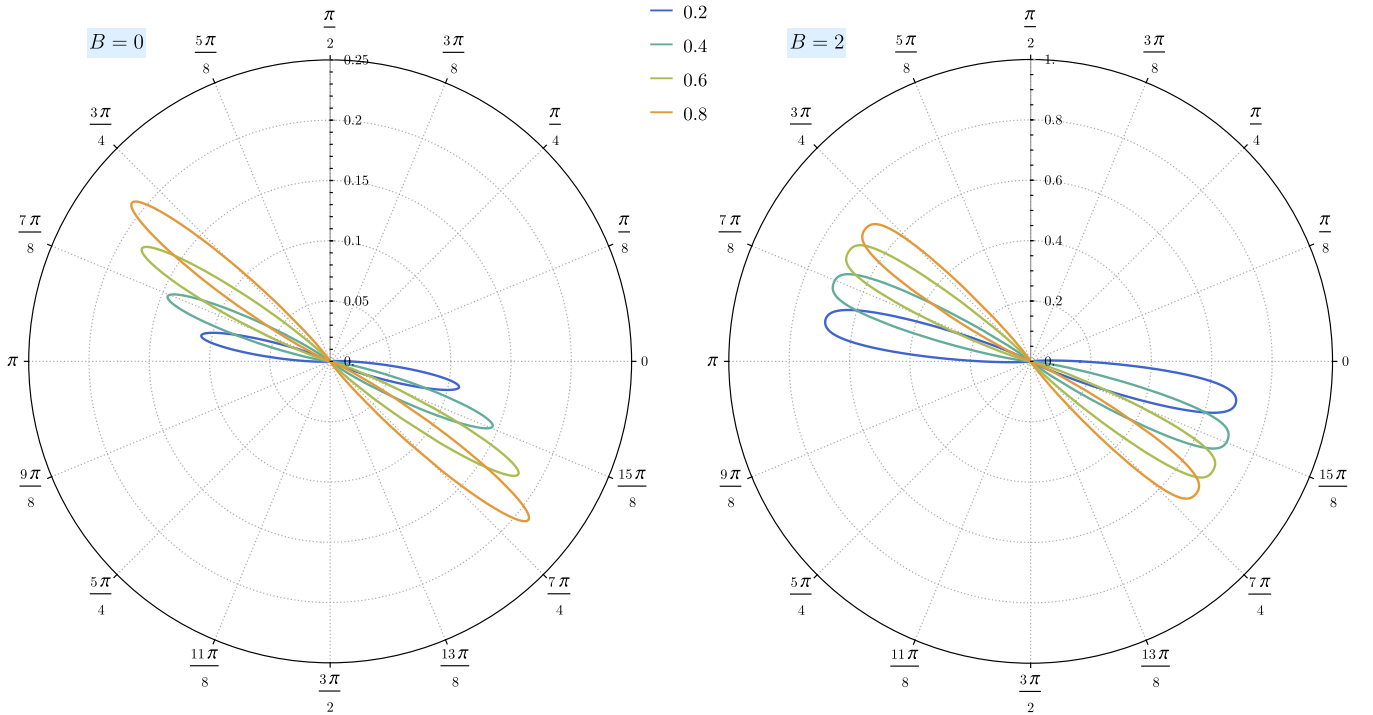


FIG. 2. Concurrence $\mathcal{C}(\varphi)$ in the polar coordinate system $r_x = r \cos \varphi$, $r_y = r \sin \varphi$, for different values of the spin-orbit constant α_e , $\alpha_e/\alpha_c = 0.2, 0.4, 0.6, 0.8$ and equally distributed spin up/down incident states $\alpha^2 = \beta^2 = 1/2$ of the itinerant electron. The value of θ : $k_x = k \cos \theta$, $k_y = k \sin \theta$, and $\theta = 5\pi/4$. The following parameters are considered: $k \equiv l_0 k = 1$, $E = 15$ meV, $r \equiv r/l_0 = 10$, and $\alpha_c = \hbar^2/m_e$, and the confinement length $l_0 = 15$ nm. The magnetic fields $B = 0$ (the left plot) and $B = 2$ T (the right plot). Different colors annotate values of α_e/α_c .

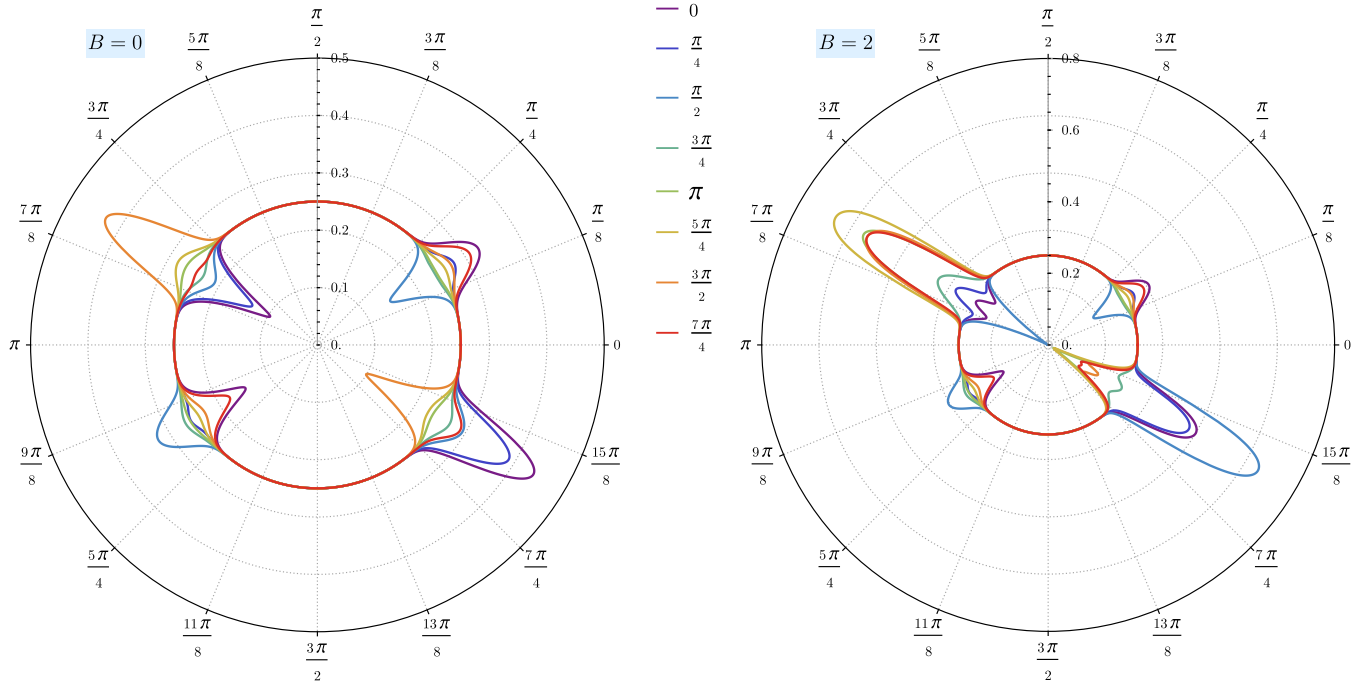


FIG. 3. Spatially anisotropic distribution of fidelity $\mathcal{F}(\varphi)$ in the polar coordinate system $r_x = r \cos \varphi$, $r_y = r \sin \varphi$, for equally distributed spin up/down incident states $\alpha^2 = \beta^2 = 1/2$ of the itinerant electron. We present results for different θ : $k_x = k \cos \theta$, $k_y = k \sin \theta$, and zero (the left plot) and nonzero magnetic fields $B = 2$ T (the right plot). The effective mass $m_e = 0.067m$ (m is the electron mass), g factor $g = -0.44$, leads to the $l_0 \approx 15$ nm. The other parameters: $\hbar\omega_0 = 4.4$ meV, $\alpha_e/\alpha_c = 0.6$, $\alpha_c = \hbar^2/m_e$, $k \equiv l_0 k = 1$, $E = 15$ meV, and $r \equiv r/l_0 = 10$. Different colors annotate values of θ .

Trace of the density matrix can be calculated through the following formula [77]:

$$\text{Tr}[\hat{\rho}^2] = \frac{1}{4} \left[1 + 3\langle (Z_u^A)^2 \rangle + 3\langle (Z_u^B)^2 \rangle + 9\langle (Z_u^{AB})^2 \rangle \right], \quad (26)$$

where

$$\begin{aligned} Z_u^A &= \text{Tr}[\hat{U}_A \hat{\rho} \hat{U}_A^\dagger \hat{\sigma}_z^A \otimes \mathcal{I}_B], \\ Z_u^B &= \text{Tr}[\hat{U}_B \hat{\rho} \hat{U}_B^\dagger \mathcal{I}_A \otimes \hat{\sigma}_z^B], \\ Z_u^{AB} &= \text{Tr}[\hat{U} \hat{\rho} \hat{U}^\dagger \hat{\sigma}_z^A \otimes \hat{\sigma}_z^B], \end{aligned} \quad (27)$$

and ensemble average moments $\langle \dots \rangle$ are done for the random SOI. Here Z_u^{AB} corresponds to the process when both spins of electrons are flipped after the scattering process, while Z_u^A and Z_u^B correspond to the processes when only one spin is flipped. After cumbersome calculations we deduce

$$\begin{aligned} \hat{U} \hat{\rho} \hat{U}^\dagger \hat{\sigma}_z^A \otimes \hat{\sigma}_z^B &= \left(\rho_{11} |0\rangle \langle 0|_A \otimes |0\rangle \langle 0|_B \right. \\ &- \rho_{22} |0\rangle \langle 0|_A \otimes |1\rangle \langle 1|_B + \rho_{44} |1\rangle \langle 1|_A \otimes |1\rangle \langle 1|_B \\ &- \rho_{12} |0\rangle \langle 0|_A \otimes |0\rangle \langle 1|_B + \rho_{14} |0\rangle \langle 1|_A \otimes |0\rangle \langle 1|_B \\ &+ \rho_{21} |0\rangle \langle 0|_A \otimes |1\rangle \langle 0|_B - \rho_{24} |0\rangle \langle 1|_A \otimes |1\rangle \langle 1|_B \\ &\left. + \rho_{41} |1\rangle \langle 0|_A \otimes |1\rangle \langle 0|_B - \rho_{42} |1\rangle \langle 0|_A \otimes |1\rangle \langle 1|_B \right). \end{aligned} \quad (28)$$

Taking into account Eq. (28) we deduce

$$Z_u^{AB} = \text{Tr}[\hat{U} \hat{\rho} \hat{U}^\dagger \hat{\sigma}_z^A \otimes \hat{\sigma}_z^B] = \rho_{11} - \rho_{22} + \rho_{44}. \quad (29)$$

If the spin of the quantum dot is frozen, similarly we obtain

$$Z_u^A = \hat{U}_A \hat{\rho} \hat{U}_A^\dagger \hat{\sigma}_z^A \otimes \mathcal{I}_B = \rho_{A11} |0\rangle \langle 0|_A \otimes |0\rangle \langle 0|_B. \quad (30)$$

As a next step we need to define mean values of squares of quantities Eq. (27). These averaged values over random $\alpha_e = \alpha_c \xi$ are defined as follows:

$$\begin{aligned} \langle (Z_u^A)^2 \rangle &= \int d\xi \mathcal{P}(\xi) (Z_u^A(\xi))^2, \\ \langle (Z_u^B)^2 \rangle &= 0, \\ \langle (Z_u^{AB})^2 \rangle &= \int d\xi \mathcal{P}(\xi) (Z_u^{AB}(\xi))^2. \end{aligned} \quad (31)$$

Here

$$\mathcal{P}(\xi) = \frac{1}{\Delta \xi \sqrt{2\pi}} \exp \left[-\frac{(\xi - \bar{\xi}_e)^2}{2(\Delta \xi)^2} \right] \quad (32)$$

is the distribution function of the random SO interaction constant v . The Renyi entropy as a function of magnetic field B is plotted in Fig. 4. As we see Renyi entropy depends on the angles θ , φ and as well as concurrence has anisotropic character. As we see the maximal values of the Renyi entropy are rotated by magnetic field B in the (k_x, k_y) plane.

VI. CONCLUSIONS

In the present work, we studied entanglement in the system of an alternating magnetic and a quantum dot. In particular, we considered the case when the itinerant electron from the alternating magnet and the electron localized in the GaAs quantum

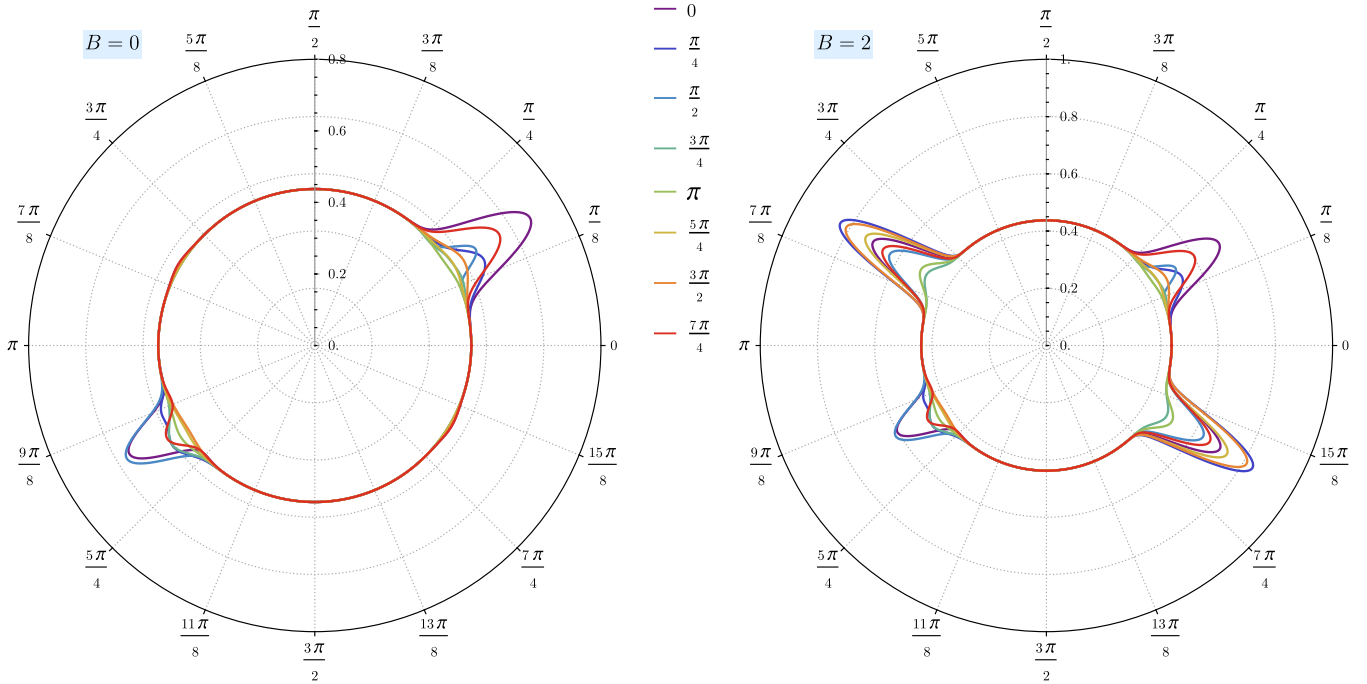


FIG. 4. Spatially anisotropic Renyi entropy $S_2(\hat{\rho}[\varphi]) = -\log_2 \text{Tr}[\hat{\rho}^2]$ in the polar coordinate system $r_x = r \cos \varphi$, $r_y = r \sin \varphi$, for equally distributed spin up/down incident states $\alpha^2 = \beta^2 = 1/2$ of the itinerant electron. The parameters of the distribution function $\mathcal{P}(\alpha_e)$: $\bar{\xi} = 1$, $\Delta\xi = 0.1$. We present results for different θ : $k_x = k \cos \theta$, $k_y = k \sin \theta$, and zero (the left plot) and nonzero magnetic fields $B = 2$ T (the right plot). The values of parameters: $k \equiv l_0 k = 1$, $E = 15$ meV, and $r \equiv r/l_0 = 10$. The confinement length $l_0 = 15$ nm. Different colors annotate values of θ .

dot doped on the altermagnet initially are disentangled and become entangled after the spin-resolved scattering process. We analytically solved coupled Lippmann-Schwinger integral equations and obtained the system's postscattering density matrix. We found that concurrence in the system is highly anisotropic and the region of nonzero concurrence rotates depending on the values of the spin-orbit constant. Realistic physical systems, in many cases, are characterized by certain disorders due to lattice dislocations and impurities. To describe the effects of the disorder, we considered the

random spin-orbit constant and calculated the Renyi entropy averaged over the randomness in the spin-orbit constant. Akin to the concurrence, the Renyi entropy also depends on the spin-orbit constant. We showed that, due to the unique properties of an altermagnetic system, tuning the applied external magnetic field allows tailoring of the desired entangled state. Thus the scattering process, in essence, mimics the $\text{CNOT}_{AB} \circ \text{Hadamard}_A$ gate transformation, converting the initial disentangled state into the entangled state of Bell's state with more than 70% fidelity.

APPENDIX: CALCULATION OF SCATTERING INTEGRALS

Fourier transformation of the wave functions Eq. (7) has the form

$$\psi_0(\mathbf{r}) = \int \frac{d^2 p}{(2\pi)^2} e^{i\mathbf{p}\cdot\mathbf{r}} \psi_0(\mathbf{p}) = \alpha e^{i\mathbf{k}\cdot\mathbf{r}} \begin{pmatrix} 1 \\ 0 \end{pmatrix} + \beta e^{i\mathbf{k}\cdot\mathbf{r}} \begin{pmatrix} 0 \\ 1 \end{pmatrix} + \alpha J \int \frac{d^2 p}{(2\pi)^2} e^{i\mathbf{p}\cdot\mathbf{r}} \frac{e^{-(\mathbf{p}-\mathbf{k})^2 l_B^2/2}}{E - E_{\mathbf{p},\uparrow} + i0} \begin{pmatrix} 1 \\ 0 \end{pmatrix}, \quad (\text{A1})$$

$$\psi_1(\mathbf{r}) = \int \frac{d^2 p}{(2\pi)^2} e^{i\mathbf{p}\cdot\mathbf{r}} \psi_1(\mathbf{p}) = \beta J \int \frac{d^2 p}{(2\pi)^2} e^{i\mathbf{p}\cdot\mathbf{r}} \frac{e^{-(\mathbf{p}-\mathbf{k})^2 l_B^2/2}}{E - 2B - E_{\mathbf{p},\downarrow} + i0} \begin{pmatrix} 0 \\ 1 \end{pmatrix}. \quad (\text{A2})$$

As we see, we have to calculate two integrals

$$I_1(\mathbf{r}) = \int \frac{d^2 p}{(2\pi)^2} e^{i\mathbf{p}\cdot\mathbf{r}} \frac{e^{-a(\mathbf{p}-\mathbf{k})^2}}{E - E_{\mathbf{p},\uparrow} + i0}, \quad (\text{A3})$$

$$I_2(\mathbf{r}) = \int \frac{d^2 p}{(2\pi)^2} e^{i\mathbf{p}\cdot\mathbf{r}} \frac{e^{-a(\mathbf{p}-\mathbf{k})^2}}{E - 2B - E_{\mathbf{p},\downarrow} + i0}, \quad (\text{A4})$$

where $a = l_B^2/2$ and $E_{\mathbf{p},\uparrow,\downarrow} = \frac{\hbar^2 p^2}{2m_e} \pm \alpha_e p_x p_y$.

Let us use an integral representation of the function

$$e^{-a(\mathbf{p}-\mathbf{k})^2} = \frac{1}{2\pi a} \int d^2 r' e^{-i(\mathbf{p}-\mathbf{k})\cdot\mathbf{r}'} e^{-r'^2/2a}. \quad (\text{A5})$$

Then we get

$$I_1(\mathbf{r}) = \frac{1}{2\pi a} \int d^2 r' e^{i\mathbf{k}\cdot\mathbf{r}'} e^{-r'^2/2a} \int \frac{d^2 p}{(2\pi)^2} \frac{e^{i\mathbf{p}\cdot(\mathbf{r}-\mathbf{r}')}}{E - E_{\mathbf{p},\uparrow} + i0}. \quad (\text{A6})$$

The integral over \mathbf{p} in Eq. (A6) is

$$\begin{aligned} I_3(\mathbf{r} - \mathbf{r}') &= \int \frac{d^2 p}{(2\pi)^2} \frac{e^{i\mathbf{p}\cdot(\mathbf{r}-\mathbf{r}')}}{E - E_{\mathbf{p},\uparrow} + i0} = \frac{1}{4\pi^2} \int dp_x dp_y \frac{e^{ip_x(r_x-r'_x)+ip_y(r_y-r'_y)}}{E - \hbar^2 p^2/2m_e - \alpha_e p_x p_y + i0} \\ &= -\frac{m_e}{2\pi^2 \hbar^2} \int_{-\infty}^{\infty} dp_y e^{ip_y(r_y-r'_y)} \int_{-\infty}^{\infty} dp_x \frac{e^{ip_x(r_x-r'_x)}}{(p_x - p_{x1})(p_x - p_{x2})}, \end{aligned} \quad (\text{A7})$$

where

$$p_{x1,2} = -\xi p_y \pm \left(\xi^2 p_y^2 - p_y^2 + \frac{2m_e E}{\hbar^2} + i0 \right)^{1/2} \quad (\text{A8})$$

and we introduced notation $\xi = \alpha_e/\alpha_c$, where $\alpha_c = \hbar^2/m_e$ is the maximum value of α_e [71]. Calculating the integral over p_x along the contour in complex p_x plane, that can be closed in the upper half plane for $r_x > r'_x$ and in the lower half plane for $r_x < r'_x$, we obtain

$$\int_{-\infty}^{\infty} dp_x \frac{e^{ip_x(r_x-r'_x)}}{(p_x - p_{x1})(p_x - p_{x2})} = \frac{2\pi i}{p_{x1} - p_{x2}} \begin{cases} e^{ip_{x1}(r_x-r'_x)}, & r_x > r'_x, \\ e^{ip_{x2}(r_x-r'_x)}, & r_x < r'_x. \end{cases} \quad (\text{A9})$$

Note that this solution will be substituted to Eq. (A6). This means that we can take in Eq. (A7) $r_x > r'_x$ as it corresponds to \mathbf{r} outside the dot. Substituting (15) with $r_x > r'_x$ to (13) we obtain

$$I_3(\mathbf{r} - \mathbf{r}') = -\frac{im_e}{2\pi \hbar^2} \int_{-\infty}^{\infty} dp_y \frac{\exp[ip_y(r_y - r'_y)] \exp[ip_{x1}(r_x - r'_x)]}{(\xi^2 p_y^2 - p_y^2 + \frac{2m_e E}{\hbar^2} + i0)^{1/2}}. \quad (\text{A10})$$

Now we can substitute Eq. (A10) into Eq. (A6):

$$\begin{aligned} I_1(\mathbf{r}) &= -\frac{im_e}{4\pi^2 \hbar^2 a} \int_{-\infty}^{\infty} dp_y \frac{\exp(ip_y r_y) \exp(ip_{x1} r_x)}{(\xi^2 p_y^2 - p_y^2 + \frac{2m_e E}{\hbar^2} + i0)^{1/2}} \int d^2 r' \exp(-r'^2/2a) \exp\{-i[(p_{x1} - k_x)r'_x + (p_y - k_y)r'_y]\} \\ &= -\frac{im_e}{2\pi \hbar^2} \int_{-\infty}^{\infty} dp_y \exp(ip_{x1} r_x + ip_y r_y) \frac{\exp\{-a[(p_{x1} - k_x)^2 + (p_y - k_y)^2]\}}{(\xi^2 p_y^2 - p_y^2 + \frac{2m_e E}{\hbar^2} + i0)^{1/2}}. \end{aligned} \quad (\text{A11})$$

If we drop $i0$ in the denominator of (13), the function under integral is divergent, but the integral convergent. Thus we can drop $i0$. Then we get

$$I_1(\mathbf{r}) = -\frac{im_e}{2\pi \hbar^2 \sqrt{1 - \xi^2}} \int_{-\infty}^{\infty} dp_y \exp(ip_{x1} r_x + ip_y r_y) \frac{\exp\{-a[(p_{x1} - k_x)^2 + (p_y - k_y)^2]\}}{\sqrt{(\kappa - p_y)(\kappa + p_y)}}, \quad (\text{A12})$$

where (we assume $E > 0$ and $\xi < 1$)

$$\kappa^2 = \frac{2m_e E}{\hbar^2(1 - \xi^2)}. \quad (\text{A13})$$

Integral Eq. (A12) can be evaluated approximately. Since we are interested in large $r \gg l_B$ (far from the dot), the main contribution in Eq. (A12) is from rather small $|p_y| < |r_y|^{-1}$. We assume $\kappa r \gg 1$. In this case, $(\kappa^2 - p_y^2)^{1/2} \simeq \kappa$ in the denominator of Eq. (A12). Besides, in the limit of $\kappa r \gg 1$, we also have $p_{x1,2} \simeq -\xi p_y \pm \kappa_0$, where $\kappa_0 = \sqrt{2m_e E}/\hbar$. Hence, from Eq. (A12), we get

$$\begin{aligned} I_1(\mathbf{r}) &\simeq -\frac{im_e e^{i\kappa_0 r_x}}{2\pi \hbar^2 \kappa_0} \int_{-\infty}^{\infty} dp_y \exp(-i\xi p_y r_x + ip_y r_y) \exp\{-a[(-\xi p_y + \kappa_0 - k_x)^2 + (p_y - k_y)^2]\} \\ &= -\frac{im_e \exp\left[i(\kappa_0 r_x - \frac{\xi r_x - r_y}{1 + \xi^2} [k_y + \xi(\kappa_0 - k_x)])\right]}{2\sqrt{\pi a}(\xi^2 + 1)\hbar^2 \kappa_0} \exp\left\{-\frac{(\xi r_x - r_y)^2 + 4a^2[\xi k_y - (\kappa_0 - k_x)]^2}{4a(\xi^2 + 1)}\right\}. \end{aligned} \quad (\text{A14})$$

Integral $I_2(\mathbf{r})$ differs from $I_1(\mathbf{r})$ by the sign of α_e . Correspondingly, we need to change the sign of ξ in (23) to get the expression for $I_2(\mathbf{r})$. Besides, we have to change $E \rightarrow E - 2B$. Thus we obtain

$$I_2(\mathbf{r}) \simeq -\frac{im_e}{2\sqrt{\pi a(\xi^2 + 1)}\hbar^2\kappa_1} \exp\left(i\left[\kappa_1 r_x + \frac{\xi r_x + r_y}{1 + \xi^2}[k_y - \xi(\kappa_1 - k_x)]\right]\right) \times \exp\left\{-\frac{(\xi r_x + r_y)^2 + 4a^2[\xi k_y + (\kappa_1 - k_x)]^2}{4a(\xi^2 + 1)}\right\}, \quad (\text{A15})$$

where $\kappa_1 = \sqrt{2m_e(E - 2B)}/\hbar$. The obtained result is valid for $\kappa r \gg 1$, $\kappa_1 r \gg 1$, and magnetic fields $B < E/2$.

-
- [1] Y. Arakawa and M. J. Holmes, Progress in quantum-dot single photon sources for quantum information technologies: A broad spectrum overview, *Appl. Phys. Rev.* **7**, 021309 (2020).
- [2] M. Prilmüller, T. Huber, M. Müller, P. Michler, G. Weihs, and A. Predojević, Hyperentanglement of photons emitted by a quantum dot, *Phys. Rev. Lett.* **121**, 110503 (2018).
- [3] D. Huber, M. Reindl, S. F. Covre da Silva, C. Schimpf, J. Martín-Sánchez, H. Huang, G. Piredda, J. Edlinger, A. Rastelli, and R. Trotta, Strain-tunable GaAs quantum dot: A nearly dephasing-free source of entangled photon pairs on demand, *Phys. Rev. Lett.* **121**, 033902 (2018).
- [4] M. Josefsson and M. Leijnse, Double quantum-dot engine fueled by entanglement between electron spins, *Phys. Rev. B* **101**, 081408(R) (2020).
- [5] D. N. Pham, S. Bharadwaj, and L. R. Ram-Mohan, Tuning spatial entanglement in interacting two-electron quantum dots, *Phys. Rev. B* **101**, 045306 (2020).
- [6] Y. Kojima, T. Nakajima, A. Noiri, J. Yoneda, T. Otsuka, K. Takeda, S. Li, S. Bartlett, A. Ludwig, A. Wieck *et al.*, Probabilistic teleportation of a quantum dot spin qubit, *npj Quantum Inf.* **7**, 68 (2021).
- [7] J. Klinovaja, D. Stepanenko, B. I. Halperin, and D. Loss, Exchange-based cnot gates for singlet-triplet qubits with spin-orbit interaction, *Phys. Rev. B* **86**, 085423 (2012).
- [8] L. Chotorlishvili, A. Gudyma, J. Wätzel, A. Ernst, and J. Berakdar, Spin-orbit-coupled quantum memory of a double quantum dot, *Phys. Rev. B* **100**, 174413 (2019).
- [9] M. Melz, J. Wätzel, L. Chotorlishvili, and J. Berakdar, Electrically tunable entanglement of an interacting electron pair in a spin-active double quantum dot, *Phys. Rev. B* **98**, 104407 (2018).
- [10] L. Chotorlishvili, A. Ernst, V. K. Dugaev, A. Komnik, M. G. Vergniory, E. V. Chulkov, and J. Berakdar, Magnetic fluctuations in topological insulators with ordered magnetic adatoms: Cr on Bi₂Se₃ from first principles, *Phys. Rev. B* **89**, 075103 (2014).
- [11] B. Trauzettel, D. V. Bulaev, D. Loss, and G. Burkard, Spin qubits in graphene quantum dots, *Nat. Phys.* **3**, 192 (2007).
- [12] M. Ezawa, A topological insulator and helical zero mode in silicene under an inhomogeneous electric field, *New J. Phys.* **14**, 033003 (2012).
- [13] M. Glazov, E. Y. Sherman, and V. Dugaev, Two-dimensional electron gas with spin-orbit coupling disorder, *Physica E* **42**, 2157 (2010).
- [14] S. Hayami, Y. Yanagi, and H. Kusunose, Bottom-up design of spin-split and reshaped electronic band structures in antiferromagnets without spin-orbit coupling: Procedure on the basis of augmented multipoles, *Phys. Rev. B* **102**, 144441 (2020).
- [15] S. Hayami, Y. Yanagi, and H. Kusunose, Spontaneous antisymmetric spin splitting in noncollinear antiferromagnets without spin-orbit coupling, *Phys. Rev. B* **101**, 220403(R) (2020).
- [16] A. Imamoglu, D. D. Awschalom, G. Burkard, D. P. DiVincenzo, D. Loss, M. Sherwin, and A. Small, Quantum information processing using quantum dot spins and cavity qed, *Phys. Rev. Lett.* **83**, 4204 (1999).
- [17] D. Loss and D. P. DiVincenzo, Quantum computation with quantum dots, *Phys. Rev. A* **57**, 120 (1998).
- [18] L. Šmejkal, J. Sinova, and T. Jungwirth, Emerging research landscape of altermagnetism, *Phys. Rev. X* **12**, 040501 (2022).
- [19] I. Mazin (The PRX Editors), Editorial: Altermagnetism—a new punch line of fundamental magnetism, *Phys. Rev. X* **12**, 040002 (2022).
- [20] Suyoung Lee, Sangjae Lee, S. Jung, J. Jung, D. Kim, Y. Lee, B. Seok, J. Kim, B. G. Park, L. Šmejkal, C.-J. Kang, and C. Kim, Broken kramers degeneracy in altermagnetic MnTe, *Phys. Rev. Lett.* **132**, 036702 (2024).
- [21] I. Turek, Altermagnetism and magnetic groups with pseudoscalar electron spin, *Phys. Rev. B* **106**, 094432 (2022).
- [22] L. Šmejkal, A. Marmodoro, K.-H. Ahn, R. González-Hernández, I. Turek, S. Mankovsky, H. Ebert, S. W. D'Souza, O. c. v. Šipr, J. Sinova, and T. c. v. Jungwirth, Chiral magnons in altermagnetic RuO₂, *Phys. Rev. Lett.* **131**, 256703 (2023).
- [23] H.-Y. Ma, M. Hu, N. Li, Jianpeng Liu, W. Yao, J.-F. Jia, and Junwei Liu, Multifunctional antiferromagnetic materials with giant piezomagnetism and noncollinear spin current, *Nat. Commun.* **12**, 2846 (2021).
- [24] I. V. Maznichenko, A. Ernst, D. Maryenko, V. K. Dugaev, E. Y. Sherman, P. Buczek, S. S. P. Parkin, and S. Ostanin, Fragile altermagnetism and orbital disorder in Mott insulator LaTiO₃, *Phys. Rev. Mater.* **8**, 064403 (2024).
- [25] L. Šmejkal, J. Sinova, and T. Jungwirth, Beyond conventional ferromagnetism and antiferromagnetism: A phase with nonrelativistic spin and crystal rotation symmetry, *Phys. Rev. X* **12**, 031042 (2022).
- [26] L. Šmejkal, A. H. MacDonald, J. Sinova, S. Nakatsuji, and T. Jungwirth, Anomalous Hall antiferromagnets, *Nat. Rev. Mater.* **7**, 482 (2022).
- [27] J. Krempaský, L. Šmejkal, S. D'souza, M. Hajlaoui, G. Springholz, K. Uhlířová, F. Alarab, P. Constantinou, V. Strocov, D. Usanov *et al.*, Altermagnetic lifting of kramers spin degeneracy, *Nature (London)* **626**, 517 (2024).
- [28] Y.-P. Zhu, X. Chen, X.-R. Liu, Y. Liu, P. Liu, H. Zha, G. Qu, C. Hong, J. Li, Z. Jiang *et al.*, Observation of plaid-like spin splitting in a noncoplanar antiferromagnet, *Nature (London)* **626**, 523 (2024).

- [29] I. I. Mazin, Altermagnetism in MnTe: Origin, predicted manifestations, and routes to detwinning, *Phys. Rev. B* **107**, L100418 (2023).
- [30] I. I. Mazin, K. Koepf, M. D. Johannes, R. González-Hernández, and L. Šmejkal, Prediction of unconventional magnetism in doped FeSb₂, *Proc. Natl. Acad. Sci. USA* **118**, e2108924118 (2021).
- [31] R. D. Gonzalez Betancourt, J. Zubáč, R. Gonzalez-Hernandez, K. Geisendorfer, Z. Šobáň, G. Springholz, K. Olejník, L. Šmejkal, J. Sinova, T. Jungwirth, S. T. B. Goennenwein, A. Thomas, H. Reichlová, J. Železný, and D. Kriegner, Spontaneous anomalous Hall effect arising from an unconventional compensated magnetic phase in a semiconductor, *Phys. Rev. Lett.* **130**, 036702 (2023).
- [32] M. Naka, Y. Motome, and H. Seo, Anomalous Hall effect in antiferromagnetic perovskites, *Phys. Rev. B* **106**, 195149 (2022).
- [33] Z. Feng, X. Zhou, L. Šmejkal, L. Wu, Z. Zhu, H. Guo, R. González-Hernández, X. Wang, H. Yan, P. Qin *et al.*, An anomalous Hall effect in altermagnetic ruthenium dioxide, *Nat. Electron.* **5**, 735 (2022).
- [34] A. Bose, N. J. Schreiber, R. Jain, D.-F. Shao, H. P. Nair, J. Sun, X. S. Zhang, D. A. Muller, E. Y. Tsymal, D. G. Schlom *et al.*, Tilted spin current generated by the collinear antiferromagnet ruthenium dioxide, *Nat. Electron.* **5**, 267 (2022).
- [35] H. Bai, L. Han, X. Y. Feng, Y. J. Zhou, R. X. Su, Q. Wang, L. Y. Liao, W. X. Zhu, X. Z. Chen, F. Pan, X. L. Fan, and C. Song, Observation of spin splitting torque in a collinear antiferromagnet RuO₂, *Phys. Rev. Lett.* **128**, 197202 (2022).
- [36] S. Karube, T. Tanaka, D. Sugawara, N. Kadoguchi, M. Kohda, and J. Nitta, Observation of spin-splitting torque in collinear antiferromagnetic RuO₂, *Phys. Rev. Lett.* **129**, 137201 (2022).
- [37] Q. Cui, B. Zeng, P. Cui, T. Yu, and H. Yang, Efficient spin Seebeck and spin Nernst effects of magnons in altermagnets, *Phys. Rev. B* **108**, L180401 (2023).
- [38] Y. Afik and J. R. M. de Nova, Quantum discord and steering in top quarks at the LHC, *Phys. Rev. Lett.* **130**, 221801 (2023).
- [39] Y. Afik and J. R. M. de Nova, Quantum information with top quarks in QCD, *Quantum* **6**, 820 (2022).
- [40] Y. Afik, Y. Kats, J. R. M. de Nova, A. Soffer, and D. Uzan, Entanglement and Bell nonlocality with bottom-quark pairs at hadron colliders, [arXiv:2406.04402](https://arxiv.org/abs/2406.04402).
- [41] K. A. Kouzakov, L. Chotorlishvili, J. Wätzel, J. Berakdar, and A. Ernst, Entanglement balance of quantum (e , $2e$) scattering processes, *Phys. Rev. A* **100**, 022311 (2019).
- [42] R. Feder, F. Giebels, and H. Gollisch, Entanglement creation in electron-electron collisions at solid surfaces, *Phys. Rev. B* **92**, 075420 (2015).
- [43] D. Vasilyev, F. O. Schumann, F. Giebels, H. Gollisch, J. Kirschner, and R. Feder, Spin-entanglement between two freely propagating electrons: Experiment and theory, *Phys. Rev. B* **95**, 115134 (2017).
- [44] S. V. Andreev, Controllable fusion of electromagnetic bosons in two-dimensional semiconductors, *Phys. Rev. B* **109**, 205423 (2024).
- [45] S. Feng, A. Agarwala, S. Bhattacharjee, and N. Trivedi, Anyon dynamics in field-driven phases of the anisotropic Kitaev model, *Phys. Rev. B* **108**, 035149 (2023).
- [46] V. Menon, N. E. Sherman, M. Dupont, A. O. Scheie, D. A. Tennant, and J. E. Moore, Multipartite entanglement in the one-dimensional spin- $\frac{1}{2}$ Heisenberg antiferromagnet, *Phys. Rev. B* **107**, 054422 (2023).
- [47] M. Kulig, P. Kurashvili, C. Jasiukiewicz, M. Inglot, S. Wolski, S. Stagraczyński, T. Masłowski, T. Szczepański, R. Stagraczyński, V. K. Dugaev, and L. Chotorlishvili, Topological insulator and quantum memory, *Phys. Rev. B* **108**, 134411 (2023).
- [48] R. W. Smaha, J. Pellicciari, I. Jarrige, V. Bisogni, A. T. Breidenbach, J. M. Jiang, J. Wen, H.-C. Jiang, and Y. S. Lee, High-energy spin excitations in the quantum spin liquid candidate Zn-substituted barlowite probed by resonant inelastic x-ray scattering, *Phys. Rev. B* **107**, L060402 (2023).
- [49] S. Wolski, M. Inglot, C. Jasiukiewicz, K. A. Kouzakov, T. Masłowski, T. Szczepański, S. Stagraczyński, R. Stagraczyński, V. K. Dugaev, and L. Chotorlishvili, Random spin-orbit gates in the system of a topological insulator and a quantum dot, *Phys. Rev. B* **106**, 224418 (2022).
- [50] P. Laurell, A. Scheie, D. A. Tennant, S. Okamoto, G. Alvarez, and E. Dagotto, Magnetic excitations, nonclassicality, and quantum wake spin dynamics in the Hubbard chain, *Phys. Rev. B* **106**, 085110 (2022).
- [51] R. Filip, Overlap and entanglement-witness measurements, *Phys. Rev. A* **65**, 062320 (2002).
- [52] P. Horodecki and A. Ekert, Method for direct detection of quantum entanglement, *Phys. Rev. Lett.* **89**, 127902 (2002).
- [53] P. Horodecki, Measuring quantum entanglement without prior state reconstruction, *Phys. Rev. Lett.* **90**, 167901 (2003).
- [54] F. Mintert and A. Buchleitner, Observable entanglement measure for mixed quantum states, *Phys. Rev. Lett.* **98**, 140505 (2007).
- [55] S. J. van Enk and C. W. J. Beenakker, Measuring $\text{Tr} \rho^n$ on single copies of ρ using random measurements, *Phys. Rev. Lett.* **108**, 110503 (2012).
- [56] A. Elben, B. Vermersch, M. Dalmonte, J. I. Cirac, and P. Zoller, Rényi entropies from random quenches in atomic Hubbard and spin models, *Phys. Rev. Lett.* **120**, 050406 (2018).
- [57] E. Y. Sherman, Minimum of spin-orbit coupling in two-dimensional structures, *Phys. Rev. B* **67**, 161303(R) (2003).
- [58] H. Häffner, W. Hänsel, C. Roos, J. Benhelm, D. Chek-al Kar, M. Chwalla, T. Körber, U. Rapol, M. Riebe, P. Schmidt *et al.*, Scalable multiparticle entanglement of trapped ions, *Nature (London)* **438**, 643 (2005).
- [59] D. Gross, Y.-K. Liu, S. T. Flammia, S. Becker, and J. Eisert, Quantum state tomography via compressed sensing, *Phys. Rev. Lett.* **105**, 150401 (2010).
- [60] B. Lanyon, C. Maier, M. Holzäpfel, T. Baumgratz, C. Hempel, P. Jurcevic, I. Dhand, A. Buyskikh, A. Daley, M. Cramer *et al.*, Efficient tomography of a quantum many-body system, *Nat. Phys.* **13**, 1158 (2017).
- [61] G. Torlai, G. Mazzola, J. Carrasquilla, M. Troyer, R. Melko, and G. Carleo, Neural-network quantum state tomography, *Nat. Phys.* **14**, 447 (2018).
- [62] R. Islam, R. Ma, P. M. Preiss, M. Eric Tai, A. Lukin, M. Rispoli, and M. Greiner, Measuring entanglement entropy in a quantum many-body system, *Nature (London)* **528**, 77 (2015).
- [63] A. M. Kaufman, M. E. Tai, A. Lukin, M. Rispoli, R. Schittko, P. M. Preiss, and M. Greiner, Quantum thermalization through entanglement in an isolated many-body system, *Science* **353**, 794 (2016).

- [64] Y.-L. Lee, Magnetic impurities in an altermagnetic metal, *Eur. Phys. J. B* **98**, 43 (2025).
- [65] G. S. Diniz and E. Vernek, Suppressed Kondo screening in two-dimensional altermagnets, *Phys. Rev. B* **109**, 155127 (2024).
- [66] P. Sukhachov and J. Linder, Impurity-induced Friedel oscillations in altermagnets and p -wave magnets, *Phys. Rev. B* **110**, 205114 (2024).
- [67] W. Chen, X. Zhou, D. Zhang, Y.-Q. Xu, and W.-K. Lou, Impurity scattering and Friedel oscillations in altermagnets, *Phys. Rev. B* **110**, 165413 (2024).
- [68] E. W. Hodt, P. Sukhachov, and J. Linder, Interface-induced magnetization in altermagnets and antiferromagnets, *Phys. Rev. B* **110**, 054446 (2024).
- [69] J. B. Tjernshaugen, M. Amundsen, and J. Linder, Crossed Andreev reflection revealed by self-consistent Keldysh-Usadel formalism, *Phys. Rev. B* **110**, 224502 (2024).
- [70] S. Giuli, C. Mejuto-Zaera, and M. Capone, Altermagnetism from interaction-driven itinerant magnetism, *Phys. Rev. B* **111**, L020401 (2025).
- [71] C. Sun and J. Linder, Spin pumping from a ferromagnetic insulator into an altermagnet, *Phys. Rev. B* **108**, L140408 (2023).
- [72] O. Gywat, G. Burkard, and D. Loss, Biexcitons in coupled quantum dots as a source of entangled photons, *Phys. Rev. B* **65**, 205329 (2002).
- [73] F. Baruffa, P. Stano, and J. Fabian, Spin-orbit coupling and anisotropic exchange in two-electron double quantum dots, *Phys. Rev. B* **82**, 045311 (2010).
- [74] G. Cordourier-Maruri, Y. Omar, R. de Coss, and S. Bose, Graphene-enabled low-control quantum gates between static and mobile spins, *Phys. Rev. B* **89**, 075426 (2014).
- [75] K. I. Kugel and D. I. Khomskĭ, The Jahn-Teller effect and magnetism: Transition metal compounds, *Sov. Phys. Usp.* **25**, 231 (1982).
- [76] W. K. Wootters, Entanglement of formation of an arbitrary state of two qubits, *Phys. Rev. Lett.* **80**, 2245 (1998).
- [77] A. Elben, B. Vermersch, C. F. Roos, and P. Zoller, Statistical correlations between locally randomized measurements: A toolbox for probing entanglement in many-body quantum states, *Phys. Rev. A* **99**, 052323 (2019).
- [78] O. Gamel, Entangled Bloch spheres: Bloch matrix and two-qubit state space, *Phys. Rev. A* **93**, 062320 (2016).